

# Optimization of Taxane Binding to Microtubules: Binding Affinity Dissection and Incremental Construction of a High-Affinity Analog of Paclitaxel

Ruth Matesanz,<sup>1,5</sup> Isabel Barasoain,<sup>1,5</sup> Chun-Gang Yang,<sup>2,3</sup> Lei Wang,<sup>2,6</sup> Xuan Li,<sup>2</sup> Concepción de Inés,<sup>1</sup> Claire Coderch,<sup>4</sup> Federico Gago,<sup>4</sup> Jesús Jiménez Barbero,<sup>1</sup> José Manuel Andreu,<sup>1</sup> Wei-Shuo Fang,<sup>2,3,7,\*</sup> and José Fernando Díaz<sup>1,7,\*</sup>

<sup>1</sup>Centro de Investigaciones Biológicas, Consejo Superior de Investigaciones Científicas, Ramiro de Maeztu 9, 28040 Madrid, Spain

<sup>2</sup>Institute of Materia Medica, Chinese Academy of Medical Sciences, 1 Xian Nong Tan Street, Beijing 100050, China

<sup>3</sup>Key Laboratory of Bioactive Substances and Resources Utilization of Chinese Herbal Medicine, Peking Union Medical College (Ministry of Education), Beijing 100050, China

<sup>4</sup>Department of Pharmacology, University of Alcalá, 28871 Alcalá de Henares, Spain

<sup>5</sup>These authors contributed equally to this work

<sup>6</sup>Present address: College of Life Sciences, Jilin University, Changchun, Jilin 130012, China

<sup>7</sup>This article is dedicated to the memory of our late colleague, Dr. Ángel R. Ortiz

\*Correspondence: wfang@imm.ac.cn (W.-S.F.), fer@cib.csic.es (J.F.D.)

DOI 10.1016/j.chembiol.2008.05.008

## SUMMARY

The microtubule binding affinities of a series of synthetic taxanes have been measured with the aims of dissecting individual group contributions and obtaining a rationale for the design of novel compounds with the ability to overcome drug resistance. As previously observed for epothilones, the positive and negative contributions of the different substituents to the binding free energies are cumulative. By combining the most favorable substitutions we increased the binding affinity of paclitaxel 500-fold. Insight into the structural basis for this improvement was gained with molecular modeling and NMR data obtained for microtubule-bound docetaxel. Taxanes with affinities for microtubules well above their affinities for P-glycoprotein are shown not to be affected by multidrug resistance. This finding strongly indicates that optimization of the ligand-target interaction is a good strategy to overcome multidrug resistance mediated by efflux pumps.

## INTRODUCTION

Cancer is one of the major causes of premature death in humans, and multidrug resistance (MDR) of neoplastic tissues is a major obstacle in cancer chemotherapy. Though many tumors initially respond favorably to chemotherapeutic treatment, effectiveness at tumor regression is limited by the development of resistance. Although several primary reasons account for MDR, the predominant cause is the overexpression and drug efflux activity of several transmembrane proteins, as best exemplified by P-glycoprotein (P-gp) (Shabbits et al., 2001).

P-gp is a member of the ATP binding cassette (ABC) family, with broad substrate specificity for substances, including anticancer drugs, peptides, and HIV protease inhibitors. It has been shown that the extent of drug resistance in human tumors correlates well with P-gp expression (Tan et al., 2000).

In a previous work with a small group of C-2 substituted cephalomannines (CPHs) (Yang et al., 2007), we noticed that the resistance indexes for high-affinity taxanes in MDR cells are much lower than those for the medium-affinity taxanes, paclitaxel (TXL) and docetaxel (DXL), used in clinical practice. These results suggest that increasing the binding affinity of these compounds might be an alternative to overcome MDR, the rationale for this being that affinity for tubulin is the main force driving the entrance of the ligand into cells.

When MDR cells are exposed to taxanes, two opposite forces control ligand uptake: (1) binding to P-gp, which pumps the ligand out of the cell, and (2) binding to tubulin, which reduces the intracellular concentration of the ligand and keeps it bound inside the cell. Thus, the higher the binding affinity of the ligand for tubulin, the lower the intracellular concentration of free ligand. Because efflux relies on drug binding to P-gp, which in turn depends on free ligand concentration, at intracellular ligand concentrations far below its dissociation constant from P-gp, the efflux will be strongly decreased. In the most extreme case of a ligand that binds covalently to the taxane site, such as the natural product cyclosporin, every molecule entering the cell will be finally trapped by tubulin, and the tumor cell's MDR phenotype will be completely circumvented (Buey et al., 2007).

Although numerous chemical and biological qualitative studies of the structure-activity relationships of taxanes have been performed (Zefirova et al., 2005; Kingston and Newman, 2007), an in-depth study of the contributions of the different substituents to the binding thermodynamics has not been conducted. We have previously shown that for epothilone (EPO) derivatives (Buey et al., 2004), the thermodynamic contributions of the substituents are accumulative, that is, the same substitution on different ligands produces a similar change on the binding affinity. The effect of a single modification can thus be quantified, and both favorable and unfavorable contributions can be combined to build tailor-made ligands with the desired affinities.

We now report on the thermodynamics of binding of a set of 44 taxanes (called Chitax [CTX]), plus the three reference compounds, TXL, DXL, and CPH (Figure 1), to crosslinked stabilized

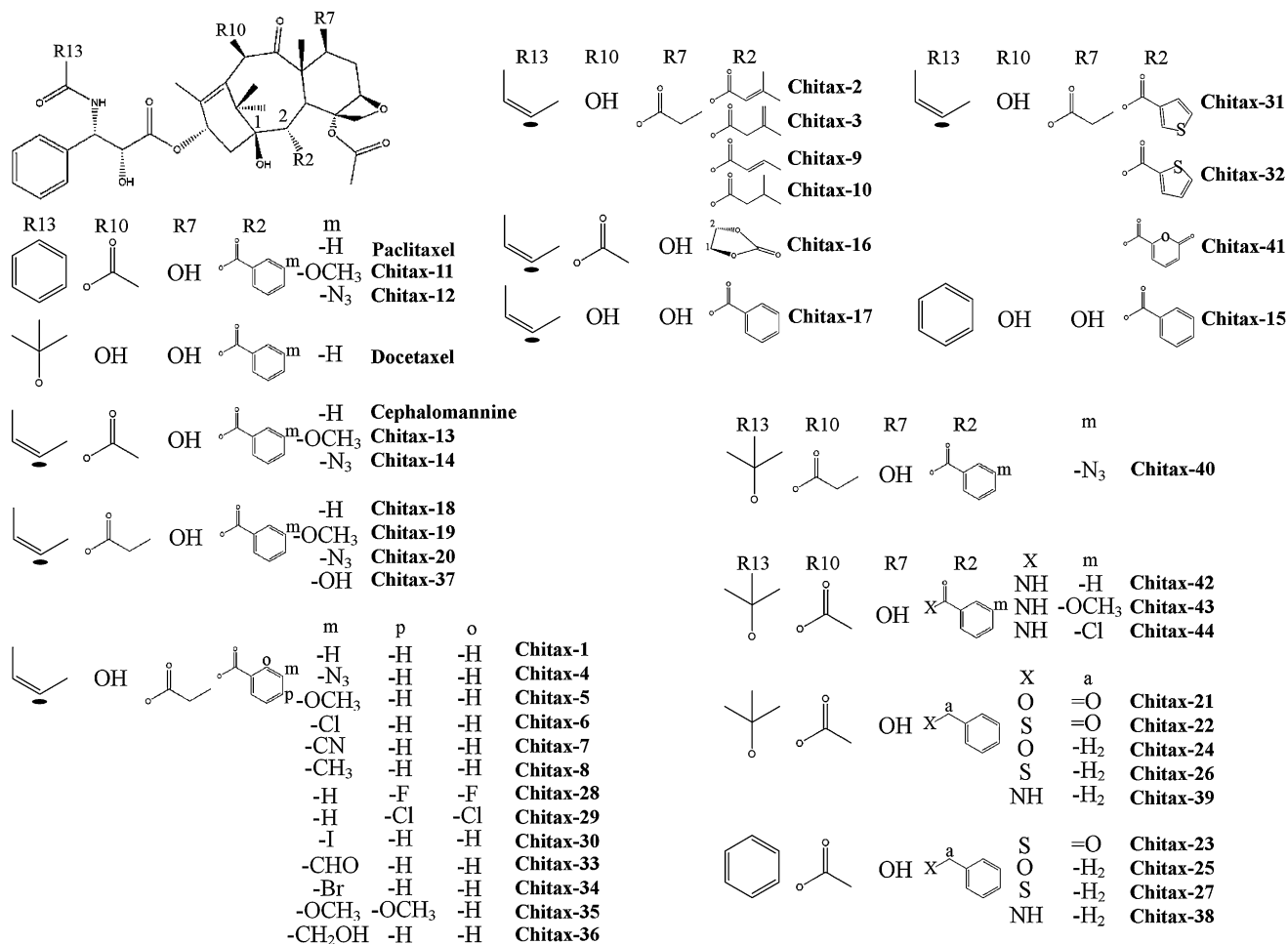


Figure 1. Chemical Structure of the Taxanes Employed in This Study

microtubules (MT) in order to quantify the contributions of single modifications at four specific locations of the taxane scaffold: two of them, C2, in the southern part of the molecule, and C13, where side chains have been described as essential for taxane activity (Chen et al., 1993b), and another two, C7 and C10, in the northern part of the molecule, where substituents have been shown as nonessential for taxane activity (Chen et al., 1993a). It is known that the side chains at these positions accept modifications that modulate the activity, favorably and unfavorably (Ojima et al., 1997; Kingston et al., 1998; Yang et al., 2007). The activity of these taxanes was investigated against the parental (A2780) and MDR P-gp-overexpressing (A2780AD) human ovarian carcinoma cell lines (Rogan et al., 1984). We were able to correlate the binding affinity of these tubulin ligands to their cytotoxicity in the resistant cells. Moreover, the resulting thermodynamic data was used to design novel high-affinity taxanes with the ability to overcome P-gp-related resistance. The higher affinity of these newly designed compounds has been rationalized by experimentally determining the tubulin bound conformation of DXL and by modeling the complexes of  $\beta$ -tubulin with DXL, TXL, and the best of the designed taxanes.

## RESULTS

### Thermodynamics of Binding of TXL Analogs to Stabilized MTs

All the compounds were first shown to be TXL-like MT-stabilizing agents (MSA) (see Table S1 available online). Then, their affinity for the taxane-binding site was measured using the competition method previously employed (Buey et al., 2004; Table 1 and Table S2). Every compound was initially measured using Flutax-2 as the competitor. Compounds 4, 11, 12, 13, 14, 19, 20, and 21 displayed very high affinities, completely displacing Flutax-2 at equimolar concentrations (Figure 2A). This indicated that they were in the limit of the range of measurement allowed by the previously employed test (Díaz and Buey, 2007).

To measure the binding affinity of these compounds more precisely, we used a direct competition experiment with a higher-affinity compound, EPO-B, whose binding affinity ( $7.5 \times 10^8 \text{ M}^{-1}$  at  $35^\circ\text{C}$ ) has been previously determined (Buey et al., 2005; Figure 2B). This allowed the precise determination of the binding affinities of compounds 4, 11, 12, 13, 14, 19, 20, and 21, whose values range between  $1.42 \times 10^8 \text{ M}^{-1}$  for the compound with the lowest affinity, CTX-21, and  $1.51 \times 10^9 \text{ M}^{-1}$  for

**Table 1. Apparent Binding Affinities, Thermodynamic Parameters of Binding of Taxanes for the TXL site,  $10^7 \text{ M}^{-1}$ , and Cytotoxicity of the Compounds to Nonresistant and Resistant Ovarian Carcinoma Cells**

Compound	Kb 35°C	$\Delta G$ 35°C kJ/mol	$\Delta H$ kJ/mol	$\Delta S$ J/mol	IC <sub>50</sub> A2780 nM	IC <sub>50</sub> A2780AD nM	R/S
TXL <sup>a</sup>	1.43 ± 0.17	-42.1 ± 0.3	-51 ± 4	-29 ± 13	1.3 ± 0.4	980 ± 149	753
DXL <sup>a</sup>	3.93 ± 0.27	-44.8 ± 0.2	-53 ± 2	-26 ± 8	0.6 ± 0.2	290 ± 16	483
CPH	0.69 ± 0.08	-40.3 ± 0.3	-39 ± 6	-6 ± 18	1.5 ± 0.2	910 ± 285	606
CTX-1	0.49 ± 0.12	-39.4 ± 0.6	-56 ± 12	-56 ± 39	13.2 ± 7	1222 ± 300	92.5
CTX-2	0.043 ± 0.018	-33.2 ± 0.9	-66 ± 18	-109 ± 38	950 ± 80	10,200 ± 1900	10.7
CTX-3	0.072 ± 0.017	-34.5 ± 0.5	-32 ± 9	10 ± 29	1250 ± 200	4000 ± 700	3.2
CTX 4 <sup>b</sup>	87 ± 19	-52.7 ± 0.5	-46 ± 13	19 ± 44	2.7 ± 0.6	14 ± 3.8	5.2
CTX-5	5.37 ± 1.39	-45.6 ± 0.6	-40 ± 4	19 ± 14	6.6 ± 1.8	160 ± 19	24.2
CTX-6	1.62 ± 0.24	-42.5 ± 0.4	-39 ± 2	13 ± 7	10 ± 2.4	274 ± 30	27.4
CTX-7	0.39 ± 0.06	-38.8 ± 0.4	-38 ± 5	4 ± 17	14.5 ± 2.9	2100 ± 660	145
CTX-8	0.492 ± 0.073	-39.4 ± 0.3	-28 ± 3	39 ± 10	22.5 ± 5	596 ± 105	26.4
CTX-9	0.028 ± 0.008	-32.1 ± 0.6	-15 ± 4	56 ± 12	3900 ± 370	15,000 ± 3500	3.8
CTX-10	0.042 ± 0.008	-33.1 ± 0.4	-12 ± 5	68 ± 18	4900 ± 600	>20000	>4
CTX 11 <sup>b</sup>	38 ± 10	-50.5 ± 0.6	-14 ± 20	117 ± 65	1.36 ± 0.2	163 ± 37	120
CTX 12 <sup>b</sup>	151 ± 3	-54.1 ± 0.1	-29 ± 9	84 ± 29	2.8 ± 0.38	42 ± 13	15
CTX 13 <sup>b</sup>	16.5 ± 2.8	-48.4 ± 0.4	-28 ± 1	66 ± 1	1.3 ± 0.2	128 ± 17	98.4
CTX 14 <sup>b</sup>	80.0 ± 2.9	-52.5 ± 0.1	-46 ± 6	21 ± 19	1.6 ± 0.3	25 ± 10	15.6
CTX-15	2.384 ± 0.53	-43.5 ± 0.5	-18 ± 11	80 ± 35	17.5 ± 2.7	5250 ± 1000	300
CTX-16	0.050 ± 0.030	-33.6 ± 1.2	-18 ± 9	49 ± 30	740 ± 100	7360 ± 750	9.9
CTX-17	0.902 ± 0.37	-41.0 ± 0.9	-24 ± 3	55 ± 10	18 ± 5.6	5412 ± 1200	301
CTX-18	1.281 ± 0.27	-41.9 ± 0.5	-22 ± 4	64 ± 14	2.1 ± 0.8	452 ± 36	215.2
CTX 19 <sup>b</sup>	14.8 ± 0.2	-48.2 ± 0.1	-48 ± 3	0 ± 9	0.54 ± 0.07	39 ± 11	72.2
CTX 20 <sup>b</sup>	80.6 ± 5.1	-52.5 ± 0.2	-92 ± 19	-124 ± 64	3.9 ± 1.2	27.4 ± 4	7
CTX 21 <sup>b</sup>	14.2 ± 1.6	-48.0 ± 0.3	-26 ± 5	72 ± 16	1.9 ± 0.3	41 ± 11	21.5
CTX-22	0.013 ± 0.00	-30.1 ± 0.0	-46 ± 7	-151 ± 23	2400 ± 1000	6960 ± 670	2.9
CTX-23	0.007 ± 0.00	-28.6 ± 0.0	-37 ± 7	-123 ± 22	11,500 ± 1000	23,800 ± 2200	2.1
CTX-24	0.094 ± 0.01	-35.2 ± 0.3	-65 ± 10	-95 ± 33	353 ± 19	8600 ± 3800	24.3
CTX-25	0.008 ± 0.00	-28.9 ± 0.0	-47 ± 7	-154 ± 24	6200 ± 2600	28,500 ± 5300	4.6
CTX-26	0.018 ± 0.00	-31.0 ± 0.0	-73 ± 11	-77 ± 137	3500 ± 1400	8300 ± 2700	2.4
CTX-27	0.007 ± 0.00	-28.6 ± 0.0	-42 ± 6	-138 ± 21	10,000 ± 740	9400 ± 1700	0.94
CTX-28	0.17 ± 0.04	-36.7 ± 0.5	-17 ± 8	62 ± 25	82 ± 16	1880 ± 200	22.9
CTX-29	0.25 ± 0.08	-37.7 ± 0.7	-52 ± 9	-48 ± 30	102 ± 8.8	690 ± 60	6.8
CTX-30	1.76 ± 0.91	-42.7 ± 1.1	-11 ± 15	92 ± 49	30 ± 0.5	246 ± 27	8.2
CTX-31	0.10 ± 0.04	-35.4 ± 0.9	-44 ± 11	-30 ± 36	106 ± 4.2	2950 ± 480	27.8
CTX-32	0.24 ± 0.08	-37.6 ± 0.7	-7 ± 16	87 ± 55	62 ± 17	3200 ± 250	51.6
CTX-33	0.07 ± 0.01	-34.4 ± 0.3	-81 ± 12	-152 ± 39	69 ± 77	1500 ± 100	21.7
CTX-34	1.20 ± 0.93	-41.7 ± 1.5	-38 ± 28	14 ± 94	28.7 ± 1.9	196 ± 14	6.8
CTX 35	0.88 ± 0.77	-40.9 ± 1.6	-29 ± 33	13 ± 112	25 ± 2	153 ± 39	6.12
CTX 36	0.029 ± 0.020	-32.2 ± 1.3	-48 ± 6	-63 ± 18	1700 ± 120	>20000	>11.7
CTX 37	0.035 ± 0.010	-32.7 ± 0.6	-91 ± 7	-207 ± 24	86 ± 9.8	10,000 ± 1000	116.2
CTX 38	0.001 ± 0.001	-23.6 ± 1.8	-44 ± 9	-70 ± 34	15,400 ± 3200	20,000 ± 3000	1.3
CTX 39	0.003 ± 0.001	-26.4 ± 0.7	-157 ± 10	-461 ± 28	4200 ± 100	5700 ± 300	1.3
CTX 40 <sup>b</sup>	628 ± 15	-57.7 ± 0.1	-26 ± 24	99 ± 80	7 ± 1	9.1 ± 0.45	1.3
CTX 41	0.021 ± 0.004	-31.4 ± 0.4	-94 ± 9	-202 ± 28	14,000 ± 2000	>20000	1.4
CTX 42	0.008 ± 0.003	-28.9 ± 0.8	-106 ± 13	-250 ± 43	192 ± 20	2750 ± 430	14.3
CTX 43	0.030 ± 0.008	-32.3 ± 0.6	-85 ± 20	-169 ± 66	69.5 ± 3.8	331 ± 70	4.8
CTX 44	0.001 ± 0.001	-23.6 ± 1.8	-177 ± 23	-493 ± 75	>20,000	>20,000	

Errors are standard errors of the mean.

<sup>a</sup> Binding affinity and thermodynamic parameters data are from Buey et al. (2004).

<sup>b</sup> Compounds measured with the EPO-B displacing method.

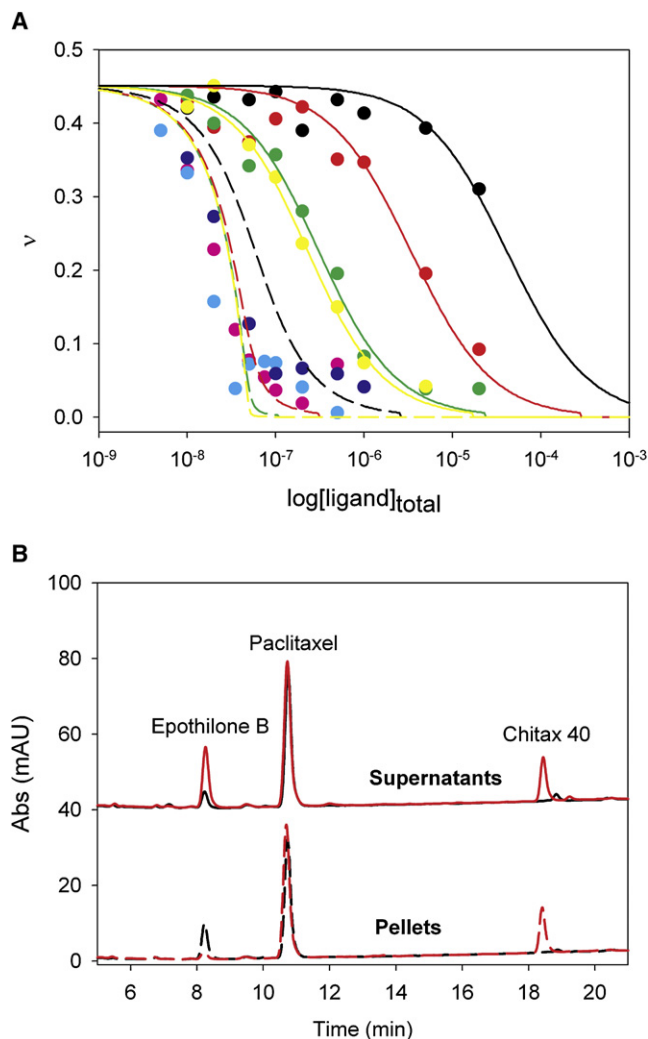


**Figure 2. Binding of the Ligands to the Paclitaxel Site**

(A) Displacement of the fluorescent taxane Flutax-2 bound to MT sites (50 nM) by taxanes at 35°C. The solid lines were generated with the best-fit value of the binding equilibrium constant of the competitors with binding affinities lower to  $10^7 \text{ M}^{-1}$ , assuming a one-to-one binding to the same site. Additional lines (dashed) show the expected displacement for ligands with binding constants of  $10^8 \text{ M}^{-1}$  (black),  $10^9 \text{ M}^{-1}$  (red),  $10^{10} \text{ M}^{-1}$  (green), and  $10^{11} \text{ M}^{-1}$  (yellow). Ligands binding data are as follows: green CPH, red CTX-2, yellow CTX-6, dark blue CTX-11, magenta CTX-12, light blue CTX-14, black CTX-27. (B) Displacement of EPO-B bound to MT sites (10  $\mu\text{M}$ ) by CTX-40 at 35°C. One micromolar TXL-binding sites were incubated with 1.1  $\mu\text{M}$  EPO-B (black lines) or with 1.1  $\mu\text{M}$  EPO-B and 1.1  $\mu\text{M}$  CTX-40 (red lines), MTs were harvested by sedimentation, ligands extracted from supernatants (solid lines) and pellets (dashed lines), and HPLC analyzed. One micromolar TXL was used as the internal standard. Supernatant traces were displaced 40 mAU for presentation purposes.

the highest-affinity compound, CTX-12. This method was validated when the binding affinities of compounds 11, 13, 19, and 21 (those in the range of  $10^8 \text{ M}^{-1}$ ) were shown to be similar using either EPO-B or Flutax-2 (see the Supplemental Data).

To confirm that the high affinity of compounds containing 3- $\text{N}_3$  benzoyl at C2 does not originate from covalent binding of its reactive azido group to  $\beta$ -tubulin, we performed experiments in

which the amounts of reversibly bound compounds 4, 12, and 14 were measured. The bound compounds could be extracted from the pellets and aqueous solutions with the aid of an organic solvent, indicating that they are not irreversibly bound.

### Molecular Modeling

One conspicuous characteristic of the taxane-binding site in  $\beta$ -tubulin (Lowe et al., 2001) is the presence of the highly exposed side chain of His229 (located in the middle of helix 7 and positionally equivalent to Arg229 in  $\alpha$ -tubulin) that splits the cavity into two major pockets. Because continuum electrostatic calculations predicted the imidazole ring of this residue to be doubly protonated at pH 6.5 ( $\text{pK}_{\text{His229}} = 7.2$ ), this ionization state was used in subsequent work.

Molecular dynamics (MD) studies of TXL, DXL, and CTX-40 in aqueous solution provided us with a range of different conformers, the most abundant of which (Figure S1) were independently studied in a first rigid-body approach by the automated docking program. The conformation previously reported for TXL (Lowe et al., 2001; Snyder et al., 2001) using either DOCK or FlexX was also found by AutoDock among the best scoring solutions. Because similar poses were found for DXL (Figure S2) and CTX-40 as well, this common disposition of the taxane in the binding site of  $\beta$ -tubulin was used in the modeling of all the complexes. Noteworthy is that these conformations are not the most populated in aqueous solution (data not shown) although they are sporadically observed in the course of transitions toward other more stable and “hydrophobically collapsed” conformations. The proposed docked conformation for TXL is then coincident with that previously found in crystals of 7-mesyl-paclitaxel, which was reportedly induced by specific interactions of the side chain at C13 with solvent (Gao and Chen, 1996).

The feasibility of the resulting modeled complexes was assessed by subjecting each of them to a 10 ns MD simulation followed by a simulated annealing procedure that provided us with a set of representative complex structures for further analysis and energy decomposition. In all cases, the ligand adopts a conformation in good agreement with the T-taxol geometry (Snyder et al., 2001; Figure 3) and is anchored in the binding site through a common set of well-defined interactions. Thus, the oxetane oxygen of the taxane is engaged in a good hydrogen bond with the NH of Thr276, whereas another hydrogen bond is established between the amide or carbamate carbonyl oxygen on the C13 substituent and the  $\text{N}_\epsilon$  of His229. The common phenyl ring at C13 (3'-Ph) establishes close van der Waals contacts with the hydrophobic side chains of Val23 and Ala233, whereas the benzoyl phenyl ring at C2 (2-OBz) gets lodged into another hydrophobic cavity, on the other side of His229, made up of the side chains of Leu217, Leu219, and Leu275. The offset stacking interaction of this latter phenyl with the imidazole ring of His229 (Figure S3) is improved by the substituent at the meta position whose 1,2- (methoxy, CTX-13) or 1,3-dipole (azide, CTX-40) additionally establishes a favorable electrostatic interaction with the amide dipole of the backbone peptide bond between His229 and Leu230 (Figure 3). Of the three hydroxyl groups that are common to the four ligands studied, that present on the C13 substituent is consistently engaged in a hydrogen bonding interaction with the carboxylate of Asp26 in helix 1 and the backbone nitrogen of Arg369, whereas that at C7 can

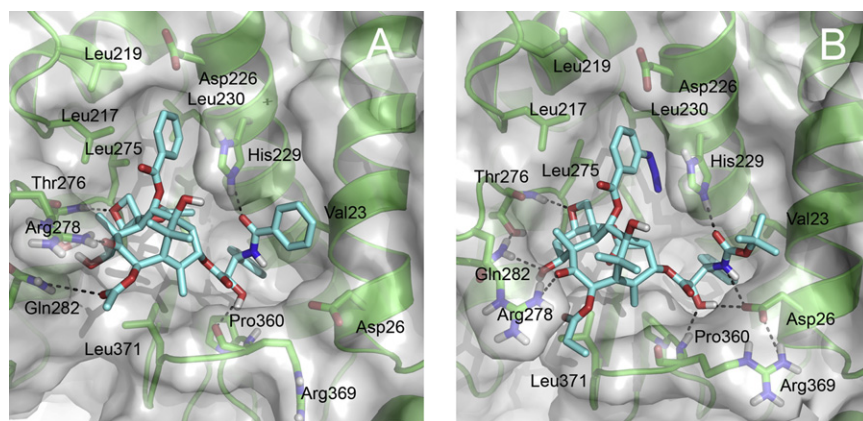


**Figure 3. Model of the Ligands Bound to the Paclitaxel Site**

(A) TXL and (B) CTX-40 in the binding site of  $\beta$ -tubulin at the end of the simulated annealing procedure. Note that the doubly protonated imidazole ring of His229 participates in (1) a hydrogen bonding interaction with the amide or carbamate carbonyl oxygen on the C13 substituent through the N $\epsilon$ , and (2) an offset stacking interaction with the phenyl ring on the C2 substituent.

establish transient hydrogen bonds with the carboxamide group of Gln282. The hydroxyl at C1 is permanently exposed to the solvent.

The four complexes yielded very low RMS deviations for the protein atoms with respect to the refined  $\beta$ -tubulin-TXL structure 1JFF ( $\sim 1.3$  Å on average for 400 atoms). The major differences when compared with this particular complex are the presence of a different rotameric state for His229, which we propose is protonated at physiological pH, and improved stacking and hydrogen bonding interactions between the ligand and the protein as a consequence of the mutual adaptation resulting from the simulated annealing procedure.

#### NMR Characterization of Bound Docetaxel

As a further step, and to provide empirical support for the modeling-derived conformations that formed the basis for the quest of the structure-activity relationship, the MT-bound conformation of DXL was elucidated, under the experimental conditions used for determining the binding constants (see the [Supplemental Data](#) file DXLNMR.pdb).

As previously shown, the transferred nuclear Overhauser enhancement (TR-NOESY) technique provides an adequate means to determine the bound conformation of ligands that exchange between free and bound states at a reasonably fast rate. TR-NOESY experiments were then performed on the DXL:MT sample at different mixing times. Negative crosspeaks were clearly observed at 310 K (Figures 4A and 4B), as expected for a ligand that binds to the assembled MTs preparation, in contrast with the lack of NOEs detected in the free state (Figure 4C).

Two control experiments were performed employing either Flutax-2 instead of DXL (the effective  $k_{\text{off}}$  of Flutax-2 release from MTs is  $1.63 \pm 0.18 \text{ s}^{-1}$  (Diaz et al., 2000) or both DXL and discodermolide (DDM) at equimolar concentrations. No TR-NOESY signals were observed in the presence of Flutax-2, indicating that the effective  $k_{\text{off}}$  of DXL is higher than that previously measured for Flutax-2, and the DXL signals were cancelled out by DDM (whose affinity for the TXL-binding site is 100 $\times$  higher), indicating that DXL is effectively bound to the TXL site (Buey et al., 2005).

#### Cytotoxicity in Resistant and Nonresistant Tumor Cells

To check the effects of the studied modifications on the cytotoxicities of the compounds and to validate the binding affinity ap-

proach as a tool to be used in ligand optimization, we performed IC<sub>50</sub> tests in A2780 human ovarian carcinoma cells and their MDR A2780AD counterparts (Table 1 and Figure 5A).

The cytotoxicities of the ligands in non-P-gp-overexpressing A2780 cells show a linear relationship ( $r = 0.81$ ) with their binding affinities, but only for those compounds with a  $\Delta G$  at 35°C higher than  $-47.5 \text{ kJ/mol}^{-1}$  ( $K_b$  at 35°C higher than  $10^8 \text{ M}^{-1}$ ), which points to a limit in the cytotoxicity that can be achieved. Thus, despite the increase in affinity of three orders of magnitude between CPH and CTX-40, the IC<sub>50</sub> remained in the order of nanomolar.

In the case of the MDR A2780AD cells, a good linear relationship ( $r = 0.80$ ) between cytotoxicities and binding affinities is observed for the full set of ligands, strongly suggesting that for these P-gp-overexpressing cells, tubulin binding is the main force competing with P-gp-mediated extrusion.

The best regression lines have slopes of 1.10 for A2780 cells and 0.61 for A2780AD cells, which indicates that P-gp-overexpression effectively reduces the intracellular drug concentration, thus making it necessary to increase the load to exert a cytotoxic effect.

#### Intake of Taxanes by Tumor Cells

The amount of compound made available for binding to the tubulin site was measured by employing radioactively labeled DXL and TXL at the concentrations needed to stop the cell cycle in G<sub>2</sub>/M, in two leukemic cell lines (U937 and K562) and the kidney epithelial nontumor cell line PtK2 from *Potorus tridactylis*. In these conditions, the intracellular drug concentration, which ranges from 0.3 to 2.8  $\mu\text{M}$  and represents a small percentage of the total drug and the cell tubulin concentrations (Table S3), increases with the total drug concentration and reaches a maximum in PtK2 cells at 300 nM DXL and 600 nM TXL. The equilibration of the ligand inside the cells is fast, with a half-life of 3 min for <sup>14</sup>C-DXL and 10 min for <sup>3</sup>H-TXL at a drug concentration of 1  $\mu\text{M}$ . The drug inside the cell was found to be in the cytoplasm, with only a small fraction bound to the nucleus, as expected.

Because the total intracellular drug concentration is more than one order of magnitude above its MT dissociation constant and much lower than the total tubulin concentration (which was considered to be  $\sim 5\%$  of the total protein measured), the mass action law dictates that most of the compound inside the cells is essentially bound to tubulin and the intracellular concentration

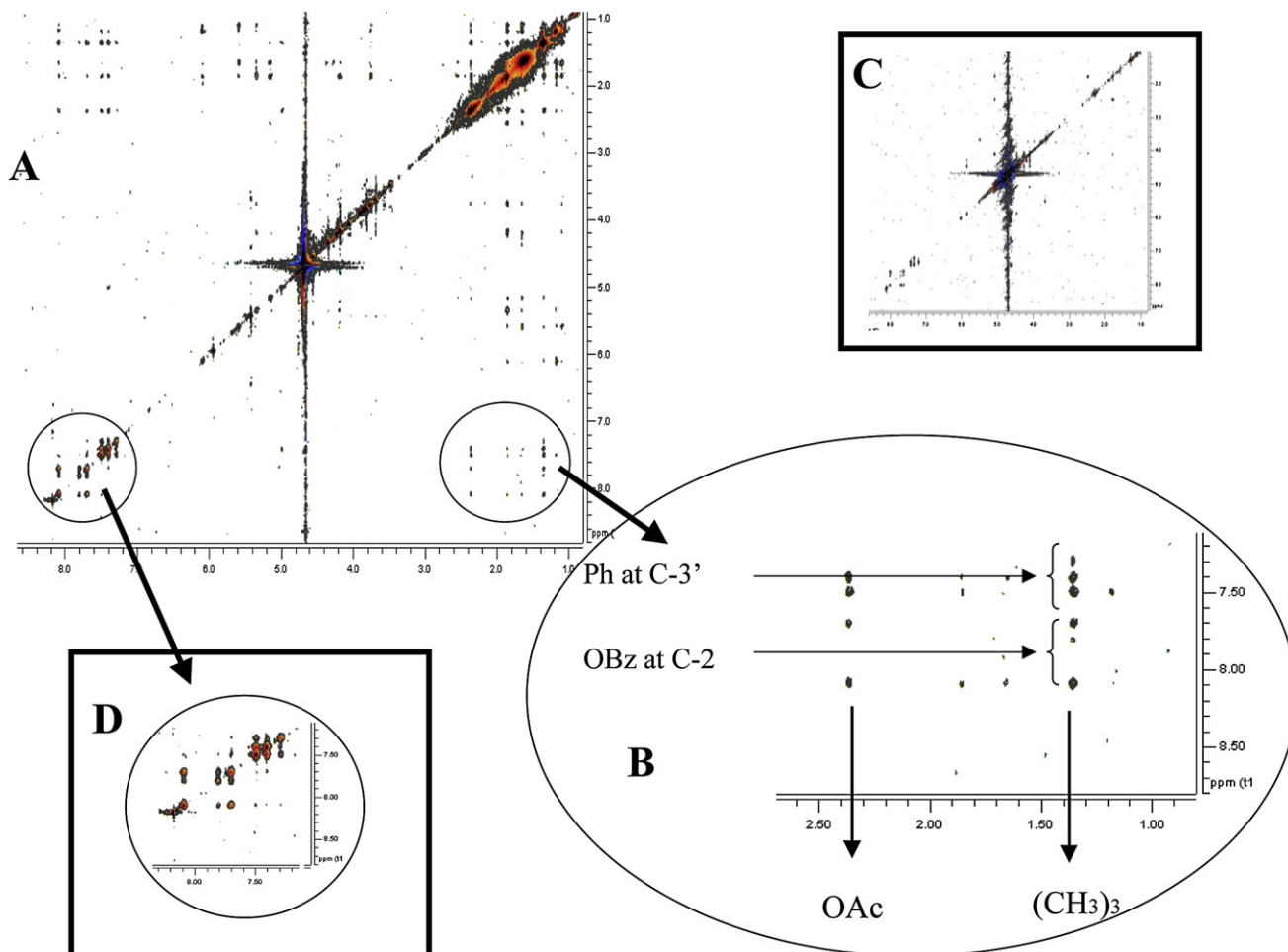


**Figure 4. NMR Characterization of the Prerelease Conformation of Bound Docetaxel**

(A) The 500 MHz TR-NOESY (mixing 200 ms, 310 K) spectrum of DXL in buffered water solution in the presence of MTs (20:1 molar ratio).

(B) Expansion showing the key TR-NOESY region: close contacts between the tert-butyl chain and the aromatic 2-OBz ring (besides the trivial crosspeaks with the vicinal 3'-Ph moiety).

(C) The NOESY experiment under the same experimental conditions (200 ms) in the absence of MTs did not show any crosspeak. (D) Expansion of the aromatic region in the TR-NOESY spectrum; no NOEs between the two aromatic 3'-Ph and 2-OBz moieties are observed.

of free drug is close to the dissociation constant (i.e., 70 nM for TXL and 25 nM for DXL).

## DISCUSSION

The effects of modifications on the substituents attached to the baccatin scaffold on the cytotoxicity of taxanes have been qualitatively discussed in several reviews (Zefirova et al., 2005; Kingston and Newman, 2007). However, the fact that these studies were performed in different cell lines precludes a rigorous evaluation of the relationship between structural changes and cytotoxicity. To quantify the effects of substitutions at a set of specific positions in a systematic way, the binding affinity for the taxane-binding site on  $\beta$ -tubulin has proved to be a more precise and objective parameter (Buey et al., 2004).

With all the binding constants determined at a given temperature (35°C), it has been possible to determine the changes in ap-

parent binding free energy caused by single-group modifications (Table 2) and to select the most favorable substituents at the positions chosen for optimization. Once this knowledge was obtained, it became feasible to design several optimized taxanes.

### Effect on Binding Affinity of Changes at the C2 Position

C2 modifications have proven to be the most effective in modulating the activity of taxanes. Thus, the 2-OBz is essential as its removal (Chen et al., 1993b) or replacement with other small side chains (Ojima et al., 1994; Nicolaou et al., 1995) results in almost total loss of activity in the human colon cancer cell line tested. In contrast, changes in the structure of the ring, including its replacement with nonaromatic or heterocyclic rings, result in only moderate losses of antitumor activity (Ojima et al., 1994). Introduction of substituents on the 2-OBz ring, (Nicolaou et al., 1994; Kingston et al., 1998; Yang et al., 2007) results in increases of activity for small groups at the meta position but loss of activity

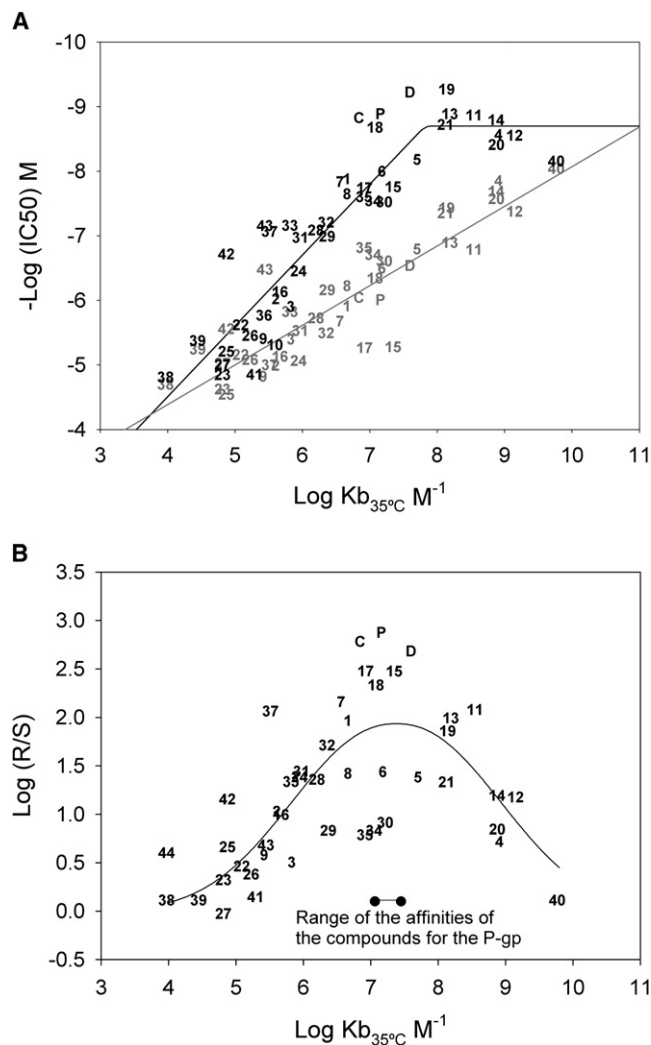


**Figure 5. Comparison between Binding Affinity and Cytotoxicity in A2780 and A2780AD Cells**

(A) Dependence of the  $IC_{50}$  of the ligands against A2780 (black) and A2780AD (gray) human ovarian carcinoma cells on the affinity for the TXL-binding site in MTs (binding constant,  $K_b$ ). The black line represents the best fit of  $IC_{50}$  against A2780 cells versus binding affinity for ligands with binding affinity under  $5 \times 10^8 \text{ M}^{-1}$ . The gray line represents the best fit of  $IC_{50}$  against A2780AD cells versus binding affinity.

(B) Dependence of the resistance index of the A2780AD MDR cells on the affinity of the compounds for the taxane binding site. The range of binding affinities of taxanes for P-gp was taken from Yang et al. (2007).

for the other positions. Changes in the linker connecting the benzene ring to the taxane core also result in decreased biological activity (Wang et al., 2007).

Our results confirm and extend the qualitative data summarized above and provide a precise quantitative characterization of the effects of C2 modifications on binding affinity:

(a) Changing the nature of the linker between the benzene ring and the taxane scaffold results in a large loss of binding free energy. Thus, the replacement of the ester by an ether, thioether, or amine moiety (compounds 24, 25, 26, 27, 38, and 39) or by a thioester or an amide (compounds 22, 23, 42, 43, and

44) results in a heavy loss of binding free energy (up to  $20 \text{ kJ/mol}^{-1}$ ). This stringent requirement indicates that the angle between the benzyl ring and the taxane core has to be strictly preserved and must be related to steric hindrance, as previously discussed for the thiobenzoyl compounds 22 and 23 (Wang et al., 2007), because the analogs in which the benzyl group is replaced by an alkyl ester (compounds 2, 3, 9, 10, and 16) only display a moderate loss of binding free energy ( $5\text{--}6 \text{ kJ/mol}^{-1}$ ), which can be assigned to the loss of interactions between the benzyl ring and the binding site.

(b) Modification of the meta substituents on the benzyl ring leads to gains of binding free energy that are the largest for  $-N_3$  ( $-11.2 \pm 1.1 \text{ kJ/mol}^{-1}$ ) and  $-OCH_3$  ( $-7.2 \pm 0.6 \text{ kJ/mol}^{-1}$ ) groups (compounds 4, 5, 11, 12, 13, 14, 20) and much smaller ( $-2\text{--}3 \text{ kJ/mol}^{-1}$ ) for halogen atoms (compounds 6, 30, and 34), whereas other small groups ( $-CN$  and  $-CH_3$ ) have no effect (compounds 7 and 8). Other similarly small substitutions ( $-OH$  and  $-CH_2OH$ ; compounds 36 and 37) are detrimental, resulting in a loss of  $7\text{--}9 \text{ kJ/mol}^{-1}$  of binding free energy.

(c) Introduction of double substituents at the 2,4 (compounds 28, 29) and 2,5 (35) positions results in loss of binding affinity. (d) The thienoyl moiety (compounds 31 and 32) can effectively replace the benzoyl group.

Because previous work from our group (Buey et al., 2004) has shown that substitutions leading to gains in binding free energy also give rise to increased cytotoxicity, the  $-N_3$  substituent at the meta position of 2-OBz was selected as the most suitable for molecule optimization.

#### Effect on Binding Affinity of Changes at the C13 Position

The side chains present at position C13 in one semisynthetic (DXL) and two natural taxanes (CPH and TXL) were evaluated to choose the optimal one for binding. Although from the direct comparison of TXL and DXL alone (Diaz and Andreu, 1993) it is not possible to assess the effect of the C13 side chain on the binding free energy due to the presence of additional differences in the substituents at C7 and C10, DXL showed a 1.9-fold larger binding affinity relative to TXL, which corresponds to a change of  $-1.6 \text{ kJ/mol}^{-1}$  in free energy of binding. A similar difference ( $2\times$ ) was observed in the cytotoxicity on 1A9 cells (Buey et al., 2005). In contrast, the tubulin binding affinity and the cytotoxicity of CPH are about  $2\times$  lower than those of DXL (Yang et al., 2007).

In our series, by comparing compounds TXL, DXL, CPH, 11, 12, 13, 14, 15, 17, 20, 21, 22, 23, 24, 25, 26, 27, 38, 39, and 40, differing only in the side chain at C13 present in the reference molecules, we can now establish that, of the three side chains, DXL provides the largest contribution to the binding free energy, ( $\Delta\Delta G \text{ C13-DXL-C13-TXL} = -3.2 \pm 0.9 \text{ kJ/mol}^{-1}$ ,  $\Delta\Delta G \text{ C13-CPH-C13-DXL} = -5.6 \pm 1.1 \text{ kJ/mol}^{-1}$ ).

#### Effect on Binding Affinity of the Substituents Present in the Northern Side of the Taxane Ring (C7 and C10)

Modifications on the northern face of TXL at positions C7 and C10 have little effect on tubulin binding, as expected from the previously described effects on cytotoxicity (Chen et al., 1993a). From all the substituents tested at C10, the best one turns out to be the propionyl group, which provides an

**Table 2. Incremental Free Energy of Binding of TXL Analogs to MTs Due to Single Group Modifications**

Modification Type	Modification	Compounds	$\Delta\Delta G$	Avg (Std Err)		
C2	Benzoyl $\rightarrow$ benzylether	T $\rightarrow$ 25	+13.2	+13.0 $\pm$ 0.2		
		21 $\rightarrow$ 24	+12.8			
	Benzoyl $\rightarrow$ benzylsulphur	T $\rightarrow$ 27	+13.6	+15.9 $\pm$ 2.3		
		21 $\rightarrow$ 26	+18.1			
	Benzoyl $\rightarrow$ benzylamine	T $\rightarrow$ 38	+18.6	+20.1 $\pm$ 1.5		
		21 $\rightarrow$ 39	+21.6			
	Benzoyl $\rightarrow$ thiobenzoyl	T $\rightarrow$ 23	+19.6	+15.9 $\pm$ 3.8		
		21 $\rightarrow$ 22	+12.1			
	Benzoyl $\rightarrow$ benzamide	21 $\rightarrow$ 42	+19.2	-3.4		
		Benzamide $\rightarrow$ 3-OCH <sub>3</sub> -benzamide	42 $\rightarrow$ 43			
	Benzamide $\rightarrow$ 3-Cl <sup>-</sup> benzamide	42 $\rightarrow$ 44	+5.3	+6.2		
	Benzoyl $\rightarrow$ 3-methyl- 2 butenoyl	1 $\rightarrow$ 2	+6.2			
	Benzoyl $\rightarrow$ 3-methyl- 3 butenoyl	1 $\rightarrow$ 3	+4.9	+7.3		
	Benzoyl $\rightarrow$ 2(E)-butenoyl	1 $\rightarrow$ 9	+7.3			
	Benzoyl $\rightarrow$ 3-methyl- butanoyl	1 $\rightarrow$ 10	+6.3	+5.8		
	Benzoyl $\rightarrow$ 2-debenzoyl-1,2-carbonate	C $\rightarrow$ 16	+5.8			
	Benzoyl $\rightarrow$ 3-N <sub>3</sub> Benzoyl	1 $\rightarrow$ 4	-8.0	-11.2 $\pm$ 1.3		
		T $\rightarrow$ 12	-13.9			
		C $\rightarrow$ 14	-12.2			
		18 $\rightarrow$ 20	-10.6			
		Benzoyl $\rightarrow$ 3-OCH <sub>3</sub> -benzoyl	1 $\rightarrow$ 5		-6.2	-7.2 $\pm$ 0.6
			T $\rightarrow$ 11		-8.3	
	C $\rightarrow$ 13		-8.1			
	Benzoyl $\rightarrow$ 3-Cl <sup>-</sup> benzoyl	18 $\rightarrow$ 19	-6.3	-3.1		
		1 $\rightarrow$ 6	-3.1			
		Benzoyl $\rightarrow$ 3-Br-benzoyl	1 $\rightarrow$ 34		-2.3	
	Benzoyl $\rightarrow$ 3-I-benzoyl	1 $\rightarrow$ 30	-3.3	+0.6		
	Benzoyl $\rightarrow$ 3-NC-benzoyl	1 $\rightarrow$ 7	+0.6			
	Benzoyl $\rightarrow$ 3-CH <sub>3</sub> -benzoyl	1 $\rightarrow$ 8	0.0	+7.2		
	Benzoyl $\rightarrow$ 3-CH <sub>2</sub> OH-benzoyl	1 $\rightarrow$ 36	+7.2			
	Benzoyl $\rightarrow$ 3-OH-benzoyl	18 $\rightarrow$ 37	+9.2	+4.8		
	3-Cl <sup>-</sup> Benzoyl $\rightarrow$ 2,4-di-Cl <sup>-</sup> benzoyl	6 $\rightarrow$ 29	+4.8			
	Benzoyl $\rightarrow$ 2,4-di-F-benzoyl	1 $\rightarrow$ 28	+2.7	+4.6		
3-OCH <sub>3</sub> -Benzoyl $\rightarrow$ 2-5-di- OCH <sub>3</sub> -benzoyl	5 $\rightarrow$ 35	+4.6				
Benzoyl $\rightarrow$ 2-thienoyl	1 $\rightarrow$ 31	+4.1	+1.8			
Benzoyl $\rightarrow$ 3-thienoyl	1 $\rightarrow$ 32	+1.8				
Benzoyl $\rightarrow$ 6-carboxy-pyran-2-one	1 $\rightarrow$ 41	+8.1	+2.0 $\pm$ 0.2			
C13 Side Chain	TXL $\rightarrow$ CPH	T $\rightarrow$ C		+1.9		
		11 $\rightarrow$ 13	+1.9			
		12 $\rightarrow$ 14	+1.6			
		15 $\rightarrow$ 17	+2.4			
	TXL $\rightarrow$ DXL	23 $\rightarrow$ 22	-1.7	-3.2 $\pm$ 0.9		
		25 $\rightarrow$ 24	-6.2			
		27 $\rightarrow$ 26	-1.3			
		38 $\rightarrow$ 39	-2.8			
	CPH $\rightarrow$ DXL	T $\rightarrow$ 21	-4.2	-5.6 $\pm$ 1.1		
		C $\rightarrow$ 21	-3.8			
17 $\rightarrow$ D		-7.7				
20 $\rightarrow$ 40		-5.2				
C10	Acetyl $\rightarrow$ -OH	T $\rightarrow$ 15	-1.3	-1.7 $\pm$ 0.8		



Table 2. Continued

Modification Type	Modification	Compounds	$\Delta\Delta G$	Avg (Std Err)
		C → 17	-0.7	
		21 → D	-3.2	
	Propionyl → -OH	18 → 17	+0.9	+0.9
	Acetyl → propionyl	C → 18	-1.6	-0.5 ± 0.4
		13 → 19	+0.2	
		14 → 20	0.0	
C7	Propionyl → -OH	17 → 1	-1.6	-1.6

Errors are standard errors of the mean.

incremental free energy change of around  $-0.5 \text{ kJ/mol}^{-1}$  over the natural C10 acetyl. In contrast, introduction of the same group at position C7 brings about a loss of  $1.6 \text{ kJ/mol}^{-1}$  of binding free energy relative to the -OH present in TXL. For this reason, a propionyl at C10 and a hydroxyl at C7 were selected as optimal substituents at these positions.

### Optimal Taxane

According to the data measured, the optimal taxane should have DXL's side chain at C13, an *m*-N<sub>3</sub>-benzoyl at C2, a propionyl at C10, and a hydroxyl at C7. Starting from compound 1, the first one in the series, with an apparent binding affinity of  $-39.4 \text{ kJ/mol}^{-1}$ , the resulting molecule should gain  $-5.6 \text{ kJ/mol}^{-1}$  from the replacement of the CPH side chain with that of DXL,  $-11.2 \text{ kJ/mol}^{-1}$  from the substitution of *m*-N<sub>3</sub>-benzoyl for benzoyl at C2,  $-1.6 \text{ kJ/mol}^{-1}$  from the change of a propionyl at C7 to a hydroxyl, and  $-0.9 \text{ kJ/mol}^{-1}$  from the change of a hydroxyl at C10 to a propionyl. Taking all of these changes together, the optimal taxane would have a predicted  $\Delta G$  at 35°C of  $-58.7 \text{ kJ/mol}^{-1}$ . When the compound was synthesized (CTX-40) and its binding affinity was measured using the EPO-B displacement method ( $K_b$ , 35°C =  $6.28 \pm 0.15 \times 10^9 \text{ M}^{-1}$ ;  $\Delta G = -57.7 \pm 0.1 \text{ kJ/mol}^{-1}$ ), the experimental value was found to be in good correspondence with the predicted value.

### Structural Interpretation of the Binding Data

Two different reasons have been proposed for the changes in activity due to modifications at C2: (1) the need for a hydrophobic group to maintain the proper taxane conformation or (2) direct interactions of the benzoyl with hydrophobic side chains of the protein (Zefirova et al., 2005). The modeling data support the view that the higher affinity of CTX-40 relative to TXL and DXL, which is mostly conferred by the phenylazide substituent present at C2, may largely stem from the simultaneous improvement of the stacking interactions with the imidazole ring of His229(+) and a better electrostatic interaction with Asp26 and Arg369 on the opposite side of the molecule, resulting from a better anchoring of the ligand in the binding site. The same rationale applies to CTX-13, which has a methoxy substituent in place of the azide, and to a lesser extent to the derivatives containing halogen atoms. As regards the methyl, cyano, hydroxyl, or hydroxymethyl substituents, they are likely to be found facing the solvent rather than orientated toward the binding pocket, thus contributing negligibly to the binding affinity, in good accord with the experimental evidence.

Likewise, the enhanced affinity contribution of the DXL and CTX-40 side-chain at C13 relative to that of TXL arises from an improved hydrogen-bonding interaction of the carbamate NH relative to the amide NH with the carboxylate of Asp26.

### Prerelease Conformation of Bound Docetaxel

Transferred NOESY signals arise from a free DXL molecule whose protons have been excited when still bound to the protein but relaxed after release from the binding site. Thus, the conformation deduced from these signals corresponds to a prerelease state of the ligand. It has been described that MT-stabilizing agents binding to the TXL site reach their luminal final location through prior transient binding to a site located in the MT pore (Diaz et al., 2003; Buey et al., 2007). Therefore the NMR structural data have to be interpreted with this caution.

Because DXT release from MT following excitation has to be fast in order to get trNOESY signals, the  $K_{off}$  of the ligand should be fast in the relaxation time scale. This is apparently in contradiction with the slow dissociation constant measured for TXL in a kinetic study,  $0.091 \pm 0.006 \text{ s}^{-1}$  (Diaz et al., 2003). This observed dissociation constant does not correspond to the release step but to the rate-limiting step of the reaction. The dissociation of taxanes from MT has been studied in detail using the fluorescent taxane derivatives Flutax-1 and Flutax-2, which dissociate from MT following a two-step mechanism (Diaz et al., 2000). The first step, which is the slower one (thus the one directly observed), has a kinetic rate constant of  $0.022 \pm 0.001 \text{ s}^{-1}$  (4-fold slower than that of TXL), whereas the second one (responsible for the release of the ligand to the medium and which can be measured only indirectly from the dependence of the kinetic rate constants on concentration) is nearly 100 times faster ( $k_{off} = 1.63 \pm 0.18 \text{ s}^{-1}$ ).

In the absence of the fluorescent probe it is not possible to calculate the value of the kinetic rate constant of the release step of DXL dissociation ( $k_{off}$ ). Control experiments with Flutax-2 performed in the same conditions did not show any trNOESY signal from this ligand, which indicates that its  $k_{off}$  value is not large enough to provide good trNOESY signals. Therefore, the effective kinetic rate of the release step of the dissociation process of DXL has to be higher. Because it is not unreasonable to think that the presence of the fluorescein moiety slows down the dissociation of Flutax-2 and the observed trNOESY crosspeaks for the DXL:MT ensemble are cancelled out by addition of DDM (a TXL-binding site ligand with a much higher affinity (Buey et al., 2005)), it can be assumed that the detected signals arise

from DXL in the last step of dissociation from MT, which may be bound to either the external site or to a modified luminal site.

The basic features of the NMR-derived conformation might be extracted from the trNOESY crosspeaks. Clear NOEs are observed between the *t*-butyl protons and the 2-OBz protons (Figure 4B), whereas only extremely weak NOEs are observed between both aromatic (2-OBz and 3'-Ph) moieties (Figure 4D). The OAc-4 group also provides NOEs with both aromatic rings (Figure 4B). These experimental observations allow us to discard the presence of the so-called "polar conformation" for DXL when this molecule is bound to MT. The NMR-derived conformation is thus basically in agreement with the conformation derived from the modeling approach (see Figure S4). And though the modeled structure is in agreement with the so-called "T-taxol geometry" (Snyder et al., 2001), the NMR-derived conformation is intermediate between this one and that dubbed collapsed geometry (Vandervelde et al., 1993). That both conformations are fairly similar and resemble the T-taxol conformation possibly indicates that the prerelease step does not largely affect the conformation of DXL, and that the T-taxol conformation is stable in the protein environment. The only observed difference is likely due to the presence of His229, which in the modeled structure is found between the 2-OBz and the C13 side chain, thus further separating these two moieties. The NMR observations are in agreement with a closer proximity between the OBz and the *t*-Bu protons (~4–5 Å) than that suggested by the modeled DXL- $\beta$ -tubulin complex (~5–6 Å). Under these constraints, the NMR-deduced prerelease bound geometry for DXL, which is close to that of T-taxol, is in agreement with that derived by the modeling procedure and resembles that described for the tubulin-bound conformation of TXL (Lowe et al., 2001), though the experimental conditions herein are markedly different.

### Binding Affinity, Cytotoxicity and P-gp-Overexpression-Mediated Multidrug Resistance

The double-log plots representing cytotoxicity versus tubulin binding affinity (Figure 5A) clearly indicate that, as in the case of EPOs and other taxane-binding site ligands, both magnitudes are related, with the binding affinity behaving as a good predictor of cytotoxicity. However, a deviation from the predicted behavior can be noted from this data. There is an apparent cytotoxicity limit ( $IC_{50} = 1$  nM) for these compounds against the non-P-gp-overexpressing cells. A review of the results from our earlier work (Buey et al., 2004, 2005) indicates that there are no MSA with an  $IC_{50}$  below nM in these cells. Despite having binding constants of the order of  $10^9$  M<sup>-1</sup>, DDM and several EPOs have  $IC_{50}$ s in the order of 1 nM or higher. In fact, *cis*-CP-tmt-EPO-B (compound 19 in Buey et al. [2004]), the compound with the highest affinity for the TXL-binding site so far described ( $2.1 \times 10^{10}$  M<sup>-1</sup>), and also the most cytotoxic ( $IC_{50} = 0.1$  nM), displays a binding affinity three orders of magnitude above that of TXL but only a 10-fold increase in cytotoxicity (Buey et al., 2004). These data suggest that a significant percentage of tubulin within the cell has to be bound to stop the cell cycle; cytotoxicity is thereby limited by the amount of compound that is needed to achieve this goal.

At the drug concentrations required to stop cell-cycle progression, the percentage of tubulin bound by the ligand is in the range of 2%–20% of the whole available protein. In the drug intake

experiments, the total amount of compound available at the concentrations needed to stop the cell cycle (or at the  $IC_{50}$ ) is around one-third (comparable) of the total amount of tubulin. Although this should be enough, in principle, for binding to a significant percentage of the protein, the results indicate that the amount of ligand available for binding to the sites is effectively much smaller (2%–10%). The reason for this might be that though all the binding sites are inside the small volume occupied by the cells, the drugs have to pass through the cell membranes and reach a threshold intracellular concentration that is opposed by the detoxification pumps. If a significant percentage (say 2%–5%) of cytoplasmic tubulin has to be bound for the taxane to exert its cytotoxicity, and the amount of ligand available for protein binding is a small percentage (2%–10%) of the total 1 nM concentrations—which is already one-third of the total amount of tubulin in the cells—it follows that for the MSA with a taxane way of action the 0.1–1 nM concentration is a limit for its cytotoxicity in cells. The same reasoning can be applied to a systemically distributed drug for which the minimal amount needed to kill the tumor cells is related to the amount of tubulin available for binding, which imposes a practical limit on the lowest dose that can be used.

However, if the goal is not to find a drug with the highest cytotoxicity possible (none of the newly synthesized high-affinity compounds has a remarkably better cytotoxicity on nonresistant cells than TXL and DXL) but rather to find one with the ability to overcome the main problem appearing in patients undergoing treatment with MSA—namely P-gp-mediated resistance—attempts to increase the affinity would seem to be steps in the right direction. Cells overexpressing P-gp are still sensitive to taxanes because they can still be killed by higher concentrations of either TXL or DXL. These very high concentrations affect normal nontumor cells as well, causing them to be differentially killed because of their inability to reduce the intracellular drug concentration, rather than differentially spared because of their lower division rate.

The data with A2780AD cells shows the expected correlation (although with a lower slope arising from their ability to reduce the intracellular drug concentration) between affinity and cytotoxicity that was previously observed for chemically related compounds (Buey et al., 2004) with no deviations being noted at the highest cytotoxicity values (9 nM for CTX-40). In this type of MDR cells the high-affinity drugs are nearly 100-fold more cytotoxic than the clinically employed taxanes (TXL and DXL) and display very low resistance indexes (as low as 1.3 for the highest-affinity derivative, CTX-40). This result was confirmed with LoVo human colon carcinoma cells and their MDR LoVo-Dox counterparts (Grandi et al., 1986; see the Supplemental Data).

When the resistance indexes of the compounds are represented against their binding affinities (Figure 5B), a bell-shaped curve is observed: the resistance index shows a maximum for taxanes displaying similar affinities for tubulin and P-gp, and then rapidly decreases when the affinity of the compound for tubulin either increases or decreases. An exception to this rule is found for compounds having a halogen atom (or a methoxy group) at the meta position of 2-OBz (CTX-5, 6, 30, 34, and 35) as they exhibit a much lower resistance index than that of other compounds with equivalent affinity.

The results confirm our previous data with other high-affinity ligands or with covalent binders (which can be considered to have infinite affinity) whose cytotoxicity is unaffected by P-gp overexpression (e.g., DDM: IC<sub>50</sub> values of 60 nM and 53 nM [I. Barasoain, unpublished data] or cyclosporin: IC<sub>50</sub> values of 43.5 nM and 51 nM [Buey et al., 2007]) against A2780 and A2780AD cells, respectively, which is a clear indication that ligands with high affinity for the taxane-binding site can overcome the P-gp-mediated MDR phenotype. The rationale for this finding is that, in these cells, the intracellular free concentration of the high-affinity binding drugs will be low (see Figures S5–S7 for a detailed mathematical model). It is clear that for the ligand to be pumped out it first has to bind to P-gp, and assuming that the kinetics of drug efflux follows a Michaelis-Menten behavior, the ligand outflow will decrease with lower free ligand concentration. Because these ligands are tightly bound to tubulin, their intracellular free concentrations are of the order of their dissociation constants, which in the case of the high-affinity compounds (K<sub>d</sub> of CTX-40 = 0.16 nM at 35°C) are far below their dissociation constants from P-gp (which range between 35 nM for TXL and 88 nM for CTX-7; Yang et al., 2007). This implies that, at concentrations able to exert cytotoxicity, the efficacy of P-gp to pump out the high-affinity compounds will be reduced by a factor between 200 and 1,000 (see the Supplemental Data). From a chemical standpoint, P-gp overexpression is irrelevant.

However, the low-affinity tubulin-binding ligands may escape the effect of the pump through a different mechanism. Because they need to reach concentrations that are much higher than those of either tubulin or P-gp to bind their target and thereby exert their cytotoxicity, the pump gets overloaded (saturated) and cannot effectively reduce the intracellular drug concentration. For this reason, these ligands act as MDR reversal agents by themselves (Brooks et al., 2003).

The present findings support the view (Buey et al., 2004, 2005) that binding affinity is the main variable to be maximized in attempts to increase the cytotoxicity of this type of compound (although on nonresistant cells a practical limit is observed at around 1 nM concentration). Additionally, high-affinity compounds can escape MDR due to P-gp overexpression by lowering the concentration of free ligand that can be pumped out by P-gp.

## SIGNIFICANCE

**The binding affinities of a series of synthetic taxanes for MTs have been measured with the aims of dissecting individual group contributions and obtaining a rationale for the design of novel compounds with the ability to overcome drug resistance. As previously observed for EPOs, the positive and negative contributions of the different substituents to the binding free energy are cumulative. By combining the most favorable substitutions in a single analog, the binding affinity was increased 500-fold over that of TXL. Insight into the structural basis for this improvement was gained when models were built that assigned an important role to the interactions of C2 and C13 substituents with the protonated side chain of His229. The relative orientation of these groups was found to be in agreement with NMR data obtained for MT-bound DXL.**

**The cytotoxicities of the compounds in ovarian carcinoma A2780 cells were found to correlate with their affinities, with an apparent cytotoxicity limit in the nanomolar range. A bell-shaped curve was obtained when the taxane resistance index was plotted versus the binding affinity showing that the P-gp-overexpressing multidrug-resistant A2780AD cells are sensitive to the highest and lowest affinity compounds, whereas resistance indexes in the range of 100 to 1,000 were obtained for those whose binding affinities for tubulin and P-gp are similar.**

**The finding that taxanes with affinities for MTs well above their affinities for P-gp are not affected by multidrug resistance strongly indicates that for a series of compounds with similar pharmacokinetic and bioavailability properties, optimization of the ligand-target interaction is a good strategy to overcome multidrug resistance mediated by efflux pumps.**

## EXPERIMENTAL PROCEDURES

### Proteins and Ligands

Purified calf brain tubulin and chemicals were as described (Diaz and Andreu, 1993). Full details of the synthesis and characterization of the ligands employed can be found in the Supplemental Data.

### Ligand-Induced Tubulin Assembly

Critical concentrations of ligand-induced tubulin assembly were measured as described (Buey et al., 2005).

### Equilibrium Binding Constants of the Ligands to MTs and Tubulin

The binding constants of the ligands with apparent binding affinities below 10<sup>8</sup> M<sup>-1</sup> for the TXL-binding site were measured as described (Buey et al., 2004). For the EPO-B method, samples of 1 ml containing 1 μM sites in glutaraldehyde-stabilized MTs, 1.1 μM EPO-B and 1.1 μM of the test compound in GAB (glycerol assembly buffer; 3.4 M glycerol, 10 mM sodium phosphate, 6 mM MgCl<sub>2</sub>, and 1 mM EGTA [pH 6.7]) with 0.1 mM GTP were incubated for 30 min at 35°C in polycarbonate centrifuge tubes (Beckman Coulter, Inc., Fullerton, CA). The samples were then centrifuged at 90,000 × g for 20 min at 35°C in a TLA-100.2 rotor employing a Beckman Optima TLX ultracentrifuge. The supernatants were collected by pipetting, and the pellets were resuspended in 10 mM phosphate buffer (pH 7.0). One micromolar TXL was added as the internal standard, except for the experiments with CTX-13 in which 1 μM DXL was used instead. Both the pellets and the supernatants were extracted three times with an excess volume of dichloromethane, dried in vacuum, and dissolved in 35 μl of methanol. The samples were analyzed by HPLC.

Reversibility of binding was checked by incubating samples containing 5 μM compounds 4, 12, or 14, and 10 μM taxoid binding sites in stabilized crosslinked MT for 30 min at 25°C in polycarbonate centrifuge tubes (Beckman) in GAB with 0.1 mM GTP (DMSO concentration was always kept under 2%). The samples were then centrifuged at 90,000 g for 10 min at 25°C in a Beckman Optima TLX ultracentrifuge with a TLA100 rotor, processed, and analyzed as described.

Binding constants for compounds reversibly displacing Flutax-2 or EPO-B were calculated using Equigra v5 (Diaz and Buey, 2007). The thermodynamic parameters (apparent ΔG<sub>0</sub>, ΔH<sub>0</sub>, and ΔS<sub>0</sub>) were calculated as described (Buey et al., 2005).

Binding of the compounds to unassembled dimeric tubulin was measured by centrifugation. Two hundred microliter samples containing 20 μM tubulin and 25 μM compound in 10 mM phosphate, 1 mM EDTA (pH 7.0) buffer (PEDTA) containing 1 mM GDP were incubated for 1 hr at 35°C in polycarbonate centrifuge tubes (Beckman). The samples were then centrifuged at 386,000 × g for 1 hr at 35°C in a TLA100 rotor employing a Beckman Optima TLX ultracentrifuge. The upper and lower 100 μl of the solution were carefully collected by pipetting, and the pellets were resuspended in 10 mM phosphate buffer (pH 7.0). The tubulin concentrations in the three samples were

measured by the Bradford assay, and 5  $\mu$ M DXL was added as the internal standard. The samples were extracted and analyzed as described.

HPLC analysis of all samples was performed in an Agilent 1100 series instrument employing a Supercosil, LC18 DB, 250  $\times$  4.6 mm, 5 mm bead diameter column developed in a gradient from 50% to 80% (v/v) acetonitrile in water at a flow rate of 1 ml/min<sup>-1</sup>, following the absorbance at  $\lambda = 220$  nm.

### Cell Biology Studies

PtK2 (kidney epithelial cell from *Potorus tridactylis*), U937 (monocytic human leukemia), K562 (myelocytic human leukemia), A2780, P-gp-overexpressing A2780AD (ovarian carcinoma) cells were cultured as described previously (Buey et al., 2005). Cytotoxicity assays were performed with the MTT assay modified as described in Yang et al. (2007).

Cell intake of <sup>3</sup>H-TXL and <sup>14</sup>C-DXL was measured as reported (Manfredi et al., 1982) with modifications, using PtK2, U937, and K562 cells. These cells, and especially the PtK2 cells, were used because they are more resistant to taxanes, and more reproducible results could be obtained. Cells were grown in 24-well plates at a density of 500,000 cells/ml (PtK2) or 300,000 cells/ml (leukemic cell lines) and were incubated in 1 ml of medium with the desired drug concentration. Supernatants were collected, and cells were washed three times with 1 ml of cold PBS and incubated overnight with 0.25 ml of NaOH 0.1 M, and then neutralized with 0.25 ml of HCl 0.1 M. The total protein concentration was determined by the Lowry method and the drug (both in the supernatants and incorporated into cells) was measured by liquid scintillation counting in a LKB 1219 spectrometer (GE Healthcare Bio-Sciences, Uppsala, Sweden). The correction for unspecific binding was determined by measuring the amount incorporated in cells preincubated with 10  $\mu$ M colchicine for 4 hr at 37°C and washed three times prior to the incubation with <sup>3</sup>H-TXL or <sup>14</sup>C-DXL. Cell volume was calculated from the volume occupied by the pellets and found to be 2.5  $\pm$  0.2, 3.96  $\pm$  0.05, and 4.3  $\pm$  0.9  $\mu$ L/10<sup>6</sup> cells for U937, K562, and PtK2, respectively.

The amounts of drugs bound to the nucleus and cytoplasm of the cells were determined as described in Simpson et al. (1987).

### Molecular Modeling

The refined structure of the  $\alpha$ , $\beta$ -tubulin dimer at 3.5 Å resolution (Lowe et al., 2001; Protein Data Bank code: 1JFF) was used for molecular modeling and ligand docking. Addition of missing hydrogen atoms and computation of the protonation state of ionizable groups in  $\beta$ -tubulin at pH 6.5 were carried out using the H<sup>+</sup> Web server (Gordon et al., 2005), which relies on AMBER (Cornell et al., 1995) force-field parameters and finite difference solutions to the Poisson-Boltzmann equation. The molecular graphics program PyMOL (DeLano Scientific, LLC, Palo Alto, CA) was employed for molecular visualization and representation. The charge distribution for the ligands studied was obtained by fitting the quantum mechanically calculated (RHF 6-31G\*\*/3-21G\*) molecular electrostatic potential (MEP) to a point charge model, as implemented in Gaussian 03 (Gaussian, Inc., Wallingford, CT). Consistent bonded and non-bonded AMBER parameters were assigned to ligand atoms in the taxanes by analogy or through interpolation from those already present in the AMBER database (ff03).

The Lamarckian genetic algorithm implemented in AutoDock 3.0.5 (Morris et al., 1998) was used to generate automated docked poses of TXL, DXL, CTX-13, and CTX-40 within the taxane-binding site by randomly changing the overall orientation of conformers from the MD ensembles that were representative of the major populations, as well as the torsion angle involving the 2-OBz.

### NMR Experiments

The NMR experiments were performed at 310 K in D<sub>2</sub>O as described (Jimenez-Barbero et al., 2006), with modifications described in the Supplemental Data, on a Bruker AVANCE 500 spectrometer (Bruker, Bruker BioSpin GmbH, Rheinstetten, Germany).

### SUPPLEMENTAL DATA

Supplemental Data include seven figures, three tables, Supplemental Experimental Procedures, Supplemental References, and two additional Supple-

mental Data files and can be found with this article online at <http://www.chembiol.com/cgi/content/full/15/6/573/DC1/>.

### ACKNOWLEDGMENTS

We thank F. Amat-Guerri for Flutax-2, K.C. Nicolaou for EPO-B, the late M. Suffness for TXL, Rhône Poulenc Rorer Aventis for DXL, and José J. Ramírez and Tulsi Pindolia for their help in the early stages of the molecular modeling work. We also thank Carne Sierra Madrid S.A. (CIF: A78074168) for providing the calf brains for tubulin purification. This work was supported in part by grant BIO2007-61336 from M.E.C. to J.F.D., BIPPED-CM from Comunidad de Madrid to F.G., J.F.D., J.J.B., and J.M.A., and grants NSFC 20572135 and MOST 2006DFA31490 to W.S.F.

Received: November 15, 2007

Revised: May 4, 2008

Accepted: May 7, 2008

Published: June 20, 2008

### REFERENCES

- Brooks, T., Minderman, H., O'Loughlin, K.L., Pera, P., Ojima, I., Baer, M.R., and Bernacki, R.J. (2003). Taxane-based reversal agents modulate drug resistance mediated by P-glycoprotein, multidrug resistance protein, and breast cancer resistance protein. *Mol. Cancer Ther.* 2, 1195–1205.
- Buey, R.M., Diaz, J.F., Andreu, J.M., O'Brate, A., Giannakakou, P., Nicolaou, K.C., Sasmal, P.K., Ritzen, A., and Namoto, K. (2004). Interaction of epothilone analogs with the paclitaxel binding site: relationship between binding affinity, microtubule stabilization, and cytotoxicity. *Chem. Biol.* 11, 225–236.
- Buey, R.M., Barasoain, I., Jackson, E., Meyer, A., Giannakakou, P., Paterson, I., Mooberry, S., Andreu, J.M., and Diaz, J.F. (2005). Microtubule interactions with chemically diverse stabilizing agents: thermodynamics of binding to the paclitaxel site predicts cytotoxicity. *Chem. Biol.* 12, 1269–1279.
- Buey, R.M., Calvo, E., Barasoain, I., Pineda, O., Edler, M.C., Matesanz, R., Cerezo, G., Vanderwal, C.D., Day, B.W., Sorensen, E.J., et al. (2007). Cyclo-streptin binds covalently to microtubule pores and luminal taxoid binding sites. *Nat. Chem. Biol.* 3, 117–125.
- Chen, S.H., Huang, S., Kant, J., Fairchild, C., Wei, J.M., and Farina, V. (1993a). Synthesis of 7-deoxytaxol and 7,10-dideoxytaxol via radical intermediates. *J. Org. Chem.* 58, 5028–5029.
- Chen, S.H., Wei, J.M., and Farina, V. (1993b). Taxol structure-activity relationships: synthesis and biological evaluation of 2-deoxytaxol. *Tetrahedron Lett.* 34, 3205–3206.
- Cornell, W.D., Cieplak, P., Bayly, C.I., Gould, I.R., Merz, K.M., Ferguson, D.M., Spellmeyer, D.C., Fox, T., Caldwell, J.W., and Kollman, P.A. (1995). A second generation force field for the simulation of proteins, nucleic acids, and organic molecules. *J. Am. Chem. Soc.* 117, 5179–5197.
- Diaz, J.F., and Andreu, J.M. (1993). Assembly of purified GDP-tubulin into microtubules induced by taxol and taxotere: reversibility, ligand stoichiometry, and competition. *Biochemistry* 32, 2747–2755.
- Diaz, J.F., and Buey, R.M. (2007). Characterizing ligand-microtubule binding by competition methods. *Methods Mol. Med.* 137, 245–260.
- Diaz, J.F., Strobe, R., Engelborghs, Y., Souto, A.A., and Andreu, J.M. (2000). Molecular recognition of taxol by microtubules. Kinetics and thermodynamics of binding of fluorescent taxol derivatives to an exposed site. *J. Biol. Chem.* 275, 26265–26276.
- Diaz, J.F., Barasoain, I., and Andreu, J.M. (2003). Fast kinetics of Taxol binding to microtubules. Effects of solution variables and microtubule-associated proteins. *J. Biol. Chem.* 278, 8407–8419.
- Gao, Q., and Chen, S.H. (1996). An unprecedented side chain conformation of paclitaxel (Taxol<sup>®</sup>): crystal structure of 7-mesylopaclitaxel. *Tetrahedron Lett.* 37, 3425–3428.
- Gordon, J.C., Myers, J.B., Folta, T., Shoja, V., Heath, L.S., and Onufriev, A. (2005). H<sup>+</sup>: a server for estimating pK<sub>a</sub>s and adding missing hydrogens to macromolecules. *Nucleic Acids Res.* 33, W368–371.

- Grandi, M., Geroni, C., and Giuliani, F.C. (1986). Isolation and characterization of a human colon adenocarcinoma cell-line resistant to doxorubicin. *Br. J. Cancer* *54*, 515–518.
- Jimenez-Barbero, J., Canales, A., Northcote, P.T., Buey, R.M., Andreu, J.M., and Diaz, J.F. (2006). NMR determination of the bioactive conformation of peryluside a bound to microtubules. *J. Am. Chem. Soc.* *128*, 8757–8765.
- Kingston, D.G., and Newman, D.J. (2007). Taxoids: cancer-fighting compounds from nature. *Curr. Opin. Drug Discov. Devel.* *10*, 130–144.
- Kingston, D.G.I., Chaudhary, A.G., Chordia, M.D., Gharpure, M., Gunatilaka, A.A.L., Higgs, P.I., Rimoldi, J.M., Samala, L., Jagtap, P.G., Giannakakou, P., et al. (1998). Synthesis and biological evaluation of 2-acyl analogues of paclitaxel (Taxol). *J. Med. Chem.* *41*, 3715–3726.
- Lowe, J., Li, H., Downing, K.H., and Nogales, E. (2001). Refined structure of  $\alpha\beta$ -tubulin at 3.5 Å resolution. *J. Mol. Biol.* *313*, 1045–1057.
- Manfredi, J.J., Parness, J., and Horwitz, S.B. (1982). Taxol binds to cellular microtubules. *J. Cell Biol.* *94*, 688–696.
- Morris, G.M., Goodsell, D.S., Halliday, R.S., Huey, R., Hart, W.E., Belew, R.K., and Olson, A.J. (1998). Automated docking using a Lamarckian genetic algorithm and an empirical binding free energy function. *J. Comput. Chem.* *19*, 1639–1662.
- Nicolaou, K.C., Couladouros, E.A., Nantermet, P.G., Renaud, J., Guy, R.K., and Wrasidlo, W. (1994). Synthesis of C-2 Taxol analogs. *Angew. Chem. Int. Ed. Engl.* *33*, 1581–1583.
- Nicolaou, K.C., Renaud, J., Nantermet, P.G., Couladouros, E.A., Guy, R.K., and Wrasidlo, W. (1995). Chemical synthesis and biological evaluation of C-2 taxoids. *J. Am. Chem. Soc.* *117*, 2409–2420.
- Ojima, I., Duclos, O., Zucco, M., Bissery, M.C., Combeau, C., Vrignaud, P., Riou, J.F., and Lavelle, F. (1994). Synthesis and structure-activity-relationships of new antitumor taxoids. Effects of cyclohexyl substitution at the C-3' and/or C-2 of taxotere (Docetaxel). *J. Med. Chem.* *37*, 2602–2608.
- Ojima, I., Kuduk, S.D., Pera, P., Veith, J.M., and Bernacki, R.J. (1997). Synthesis and structure-activity relationships of nonaromatic taxoids: effects of alkyl and alkenyl ester groups on cytotoxicity. *J. Med. Chem.* *40*, 279–285.
- Rogan, A.M., Hamilton, T.C., Young, R.C., Klecker, R.W., and Ozols, R.F. (1984). Reversal of adriamycin resistance by verapamil in human ovarian cancer. *Science* *224*, 994–996.
- Shabbits, J.A., Krishna, R., and Mayer, L.D. (2001). Molecular and pharmacological strategies to overcome multidrug resistance. *Expert Rev. Anticancer Ther.* *1*, 585–594.
- Simpson, R.U., Hsu, T., Begley, D.A., Mitchell, B.S., and Alizadeh, B.N. (1987). Transcriptional regulation of the C-Myc protooncogene by 1,25-dihydroxyvitamin-D<sub>3</sub> in HL-60 promyelocytic leukemia cells. *J. Biol. Chem.* *262*, 4104–4108.
- Snyder, J.P., Nettles, J.H., Cornett, B., Downing, K.H., and Nogales, E. (2001). The binding conformation of Taxol in  $\beta$ -tubulin: a model based on electron crystallographic density. *Proc. Natl. Acad. Sci. USA* *98*, 5312–5316.
- Tan, B., Piwnicka-Worms, D., and Ratner, L. (2000). Multidrug resistance transporters and modulation. *Curr. Opin. Oncol.* *12*, 450–458.
- Vandervelde, D.G., Georg, G.I., Grunewald, G.L., Gunn, G.W., and Mitscher, L.A. (1993). "Hydrophobic collapse" of taxol and taxotere solution conformations in mixtures of water and organic solvent. *J. Am. Chem. Soc.* *115*, 11650–11651.
- Wang, L., Alcaraz, A.A., Matesanz, R., Yang, C.G., Barasoain, I., Díaz, J.F., Li, Y.Z., Snyder, J.P., and Fang, W.S. (2007). Synthesis, biological evaluation, and tubulin binding poses of C-2a sulfur linked taxol analogues. *Bioorg. Med. Chem. Lett.* *17*, 3191–3194.
- Yang, C.G., Barasoain, I., Li, X., Matesanz, R., Liu, R., Sharom, F.J., Diaz, J.F., and Fang, W. (2007). Overcoming tumor drug resistance mediated by P-glycoprotein overexpression with high affinity taxanes: a SAR study of C-2 modified 7-acyl-10-deacetyl cephalomannines. *ChemMedChem* *2*, 691–701.
- Zefirova, O.N., Nurieva, E.V., Ryzhov, A.N., Zyk, N.V., and Zefirov, N.S. (2005). Taxol: synthesis, bioactive conformations, and structure-activity relationships in its analogs. *Russ. J. Org. Chem.* *41*, 315–351.